NASA/TM-2001-211258

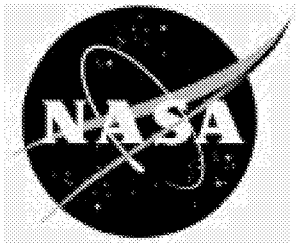

Comparison of Thermal Coefficients for Two Microwave Detectors

Diode/Voltage-to-Frequency Converter and Flash Analog-to-Digital Converter

Anne I. Mackenzie
Langley Research Center, Hampton, Virginia

December 2001

The NASA STI Program Office . . . in Profile

Since its founding, NASA has been dedicated to the advancement of aeronautics and space science. The NASA Scientific and Technical Information (STI) Program Office plays a key part in helping NASA maintain this important role.

The NASA STI Program Office is operated by Langley Research Center, the lead center for NASA's scientific and technical information. The NASA STI Program Office provides access to the NASA STI Database, the largest collection of aeronautical and space science STI in the world. The Program Office is also NASA's institutional mechanism for disseminating the results of its research and development activities. These results are published by NASA in the NASA STI Report Series, which includes the following report types:

- TECHNICAL PUBLICATION. Reports of completed research or a major significant phase of research that present the results of NASA programs and include extensive data or theoretical analysis. Includes compilations of significant scientific and technical data and information deemed to be of continuing reference value. NASA counterpart of peer-reviewed formal professional papers, but having less stringent limitations on manuscript length and extent of graphic presentations.

- TECHNICAL MEMORANDUM. Scientific and technical findings that are preliminary or of specialized interest, e.g., quick release reports, working papers, and bibliographies that contain minimal annotation. Does not contain extensive analysis.

- CONTRACTOR REPORT. Scientific and technical findings by NASA-sponsored contractors and grantees.

- CONFERENCE PUBLICATION. Collected papers from scientific and technical conferences, symposia, seminars, or other meetings sponsored or co-sponsored by NASA.

- SPECIAL PUBLICATION. Scientific, technical, or historical information from NASA programs, projects, and missions, often concerned with subjects having substantial public interest.

- TECHNICAL TRANSLATION. English-language translations of foreign scientific and technical material pertinent to NASA's mission.

Specialized services that complement the STI Program Office's diverse offerings include creating custom thesauri, building customized databases, organizing and publishing research results . . . even providing videos.

For more information about the NASA STI Program Office, see the following:

- Access the NASA STI Program Home Page at *http://www.sti.nasa.gov*

- Email your question via the Internet to help@sti.nasa.gov

- Fax your question to the NASA STI Help Desk at (301) 621-0134

- Telephone the NASA STI Help Desk at (301) 621-0390

- Write to:
  NASA STI Help Desk
  NASA Center for AeroSpace Information
  7121 Standard Drive
  Hanover, MD 21076-1320

NASA/TM-2001-211258

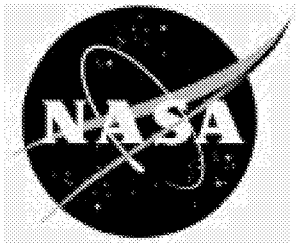

Comparison of Thermal Coefficients for Two Microwave Detectors

Diode/Voltage-to-Frequency Converter and Flash Analog-to-Digital Converter

Anne I. Mackenzie
Langley Research Center, Hampton, Virginia

National Aeronautics and
Space Administration

Langley Research Center
Hampton, Virginia 23681-2199

December 2001

Acknowledgments

This work was performed by the Passive Sensors Group in the Sensors Research Branch at the NASA Langley Research Center. Thanks to Roland W. Lawrence and William L. Munden for sharing their technical ideas, to William L. Munden for setting up the noise source, to Terry L. Mack for building the diode/VFC detector, and to Michael J. Scherner for obtaining the other new components necessary to perform the experiment. Also, thanks to Fred D. Fitzpatrick of the Flight Instrumentation Branch for the loan of the logic analyzer.

Available from:

NASA Center for AeroSpace Information (CASI)
7121 Standard Drive
Hanover, MD 21076-1320
(301) 621-0390

National Technical Information Service (NTIS)
5285 Port Royal Road
Springfield, VA 22161-2171
(703) 605-6000

Contents

Nomenclature

ADC	analog-to-digital converter
B	bandwidth
BPF	bandpass filter
CW	continuous wave
dc	direct current
G	gain
GPIB	general purpose interface bus
I	current
$k_{\text{Boltzmann}}$	Boltzmann's constant, $1.381 \times \geq 10^{-23}$ J/K
LPF	lowpass filter
MEMS	mesh emissivity measurement system
MMIC	microwave and millimeter wave integrated circuit
P	power
PC	personal computer
PMMW	passive millimeter wave
ppt	parts per thousand
RF	radio frequency
rms	root mean square
SNR	signal to noise power ratio
TC	thermal coefficient
TEC	thermoelectric cooler
VFC	voltage-to-frequency converter
Z	impedance

Abstract

Laboratory measurements were performed to compare the thermal coefficients of two microwave detectors that might be used for direct detection in L-band radiometers. In particular it was desired to compare the performance of a new-technology flash ADC (analog-to-digital converter) against that of an older-technology diode detector in series with a VFC (voltage-to-frequency converter). The outputs of two state-of-the-art detectors were recorded as a constant 1.414-GHz signal was input and the physical temperatures of the detectors were varied over a range of 10°C. As a further experiment, each detector was tested with a noise diode source and with a sine wave synthesizer source. Thermal coefficients were computed in terms of W/°C and in terms of ppt/°C at nominal operating temperatures reasonable for the individual devices. Finally, thermal coefficients were calculated in K/°C to indicate the change in brightness temperature seen by a theoretical sea surface salinity radiometer employing each detector. The K/°C for the flash ADC was determined to be about 2.8 times that of the diode/VFC. Different reactions of the ADC to a noise input and a sine wave input indicated that ADC tests for radiometric purposes, such as this one, should be performed using a noise input.

Introduction

Since the 1970s, microwave radiometer front-end hardware has been simplified by the use of direct detection, that is, detection of energy without heterodyning to produce an intermediate frequency. One direct detection device readily available for frequencies up to 50 GHz is the square law, microwave frequency diode detector, which generates an analog output dc voltage proportional to the detected input power of the diode. The Langley Salinity Mapper (ref. 1) used such a diode detector for sea surface temperature and salinity mapping at the L-band frequency in 1976. In that year, the instrument collected data during flights over the lower Chesapeake Bay and adjacent Atlantic Ocean. Recent examples at Langley include the 4.3-GHz Precision Radiometer used for stability measurements in the laboratory (ref. 2) and an Airborne C-band (6.8 GHz) Microwave Radiometer prototype used for experiments with digital averaging, also in the laboratory (ref. 3).

Work with detector diodes has shown them to be among the more temperature-sensitive front-end components. The desire for improved resolution has led to the incorporation of the planar-doped tunnel diode, known for superior thermal stability, and elaborate temperature control systems in receiver designs. MEMS (mesh emissivity measurement system) (ref. 4) operating at L-band and at C-band frequencies is a sky bucket radiometer at Langley that uses a planar-doped tunnel diode for measuring the emissivities of antenna mesh materials. MEMS and the near 20-GHz advanced water vapor radiometer prototype (ref. 5) at the Jet Propulsion Laboratory are examples of radiometers with which great care has been taken with the temperature control system.

Another direct detector technology currently under development, but which will not be further discussed in this report, is the MMIC (microwave and millimeter wave integrated circuit) chip (ref. 6). Focal plane arrays of these chips are being used to build passive imaging sensors for measurements at up to 220 GHz. One such example is the 94-GHz PMMW (passive millimeter wave) camera being developed by TRW Enterprises, Inc. (ref. 7).

Areas of current scientific interest, such as salinity mapping, require still more resolution at L-band frequencies than what has been previously achieved. For example, identification of sea surface salinity to within 0.1 part per thousand (ppt) requires a radiometric resolution of 0.05 K. Therefore, a microwave detector with greater thermal stability would be advantageous, allowing improved radiometric resolution in addition to improved accuracy and less frequent calibration through decreased drift.

With the realization of flash ADCs with high analog bandwidths (up to 2.2 GHz at the time of this study), the ADC has become another possible direct detection device for radiometry (ref. 8). The ADC is a compact device that directly outputs a digitized counts value proportional to the detected voltage input at L-band. The flash ADC contains a bank of comparators, one for each bit. Upon command, the comparators convert the sampled energy to a binary word, all in one step—hence the title "flash."

A laboratory experiment was performed by the Sensors Research Branch at the Langley Research Center to compare the thermal coefficients of a state-of-the-art microwave diode detector in series with a VFC and a state-of-the-art flash ADC. That is, it was determined whether the ADC, compared with a diode detector, was responsive to brightness temperatures in a manner less dependent on the physical temperature of the detector itself. The two detectors temperature tested were (1) a MICA DTN 4080 M1 diode in series with a Burr-Brown 110 VFC and (2) a MAXIM MAX106 ADC evaluation kit. These are depicted by simplified block diagrams in figure 1.

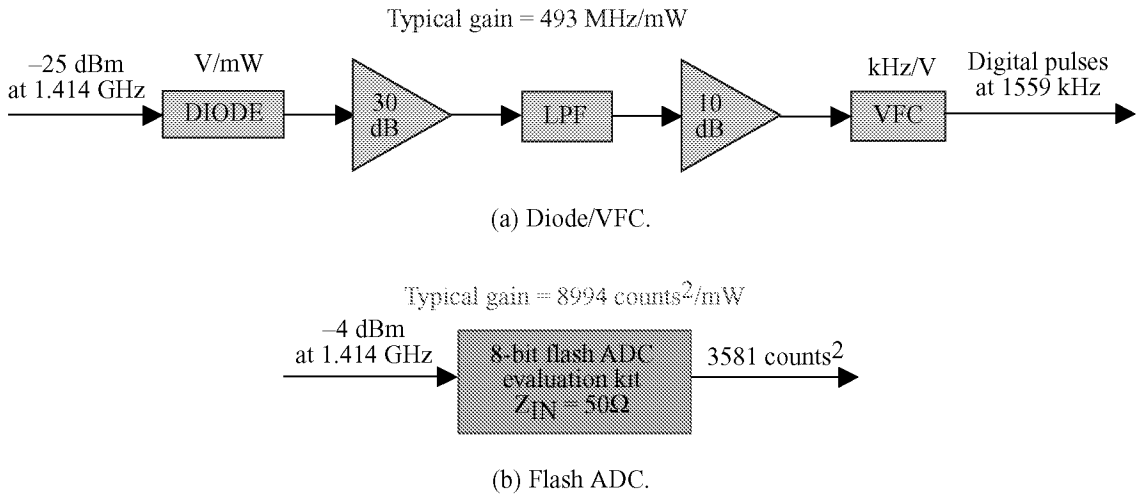

Figure 1. Simplified block diagram of microwave detectors for which thermal coefficients were measured, shown with gains typical for noise inputs.

A secondary experiment was performed to find out if the thermal coefficients of the detectors were different for sine wave inputs than for noise inputs. A noise diode more closely simulates the naturally occurring L-band noise detected by a radiometer. However, a sine wave synthesizer is more convenient to set up and would be preferable in laboratory tests if it produced the same results.

The following sections describe the fundamental differences between the two detectors, the experimental setup, the calculation methods, and the results of the thermal tests.

Characteristics of the Detectors

Although this study addressed only thermal coefficient differences between the two detector types, there were other noteworthy differences that should be considered in designing an L-band radiometer. The diode/VFC produced an analog output, while the ADC produced a digital output. Because the maximum digital sampling rate of the ADC was 600 MHz, which was less than twice the frequency of interest, a technique called bandpass sampling of the ADC was employed. In bandpass sampling, a sampling rate is chosen to intentionally alias the L-band noise to a much lower intermediate frequency where it can be correctly detected. For the study, the sampling frequency was 60 MHz. An excellent discussion of bandpass sampling, including how to calculate the intermediate frequency, is given by Akos and Tsui (ref. 9).

The diode detector output was directly proportional to power. According to its analog bandwidth of 100 MHz, the diode automatically averaged its own results. (A frequency counter did further digital averaging after the VFC stage.) The ADC output was directly proportional to voltage; the rms (root mean square) power detected by the ADC, therefore, was calculated from a series of recorded voltages long enough to include many thousands of 1.414-GHz cycles.

To obtain a linear response from the diode, it was provided with –25 dBm of power, a level in the middle of the diode functional range. Obtaining good sensitivity from the ADC dictated that it be provided with a power level close to the upper limit for the device (0 dBm). However, the ADC with a bandwidth of 2.2 GHz, when used for detecting 1.414-GHz noise, was operating near the high limit of its useful frequency range. In this region, the operating characteristics such as SNR (signal to noise power ratio) were known to deteriorate with very high power levels, and it was decided to back off from 0 to –4 dBm. At this level, the graphical display of the ADC output showed no voltage peaks being cut off. For the study, the input noise power provided to the diode/VFC was therefore amplified by 21 dB less than the noise power provided to the ADC.

The physical operating temperature range of the diode/VFC was –40° to 85°C; for the experiment it was operated at physical temperatures between 20° and 30°C. The ADC die operating range was from 80° to 150°C; for the experiment it was operated between 100° and 110°C. This characteristic of running hot compared with the diode/VFC meant that the ADC required more power. Consequently, the temperature control system for an ADC-based radiometer would itself require more power.

Experimental Setup

Setup and Measurement Procedure for the Diode/VFC Detector Test

The experimental setup for the diode/VFC thermal test is shown in a block diagram in figure 2. Appendix A lists more detailed part and instrument names.

The detector diode, op amps, lowpass filter, and VFC were fastened to a thermally regulated aluminum plate that was mounted inside an aluminum case. A temperature controller exterior to the detector case sensed the physical temperature of the plate by means of a thermistor. Using four thermoelectric coolers on the underside of the plate, the controller maintained a uniform physical temperature on the plate, according to the manual setting on the controller. During thermal tests, the controller setting was changed in 1° steps from 20° to 30°C. The physical temperature of the detector plate was allowed to stabilize for 5 min before detector output data were collected. The pulses emitted by the VFC were shaped and input to a frequency counter, which averaged the results for two 100-sec periods. At each

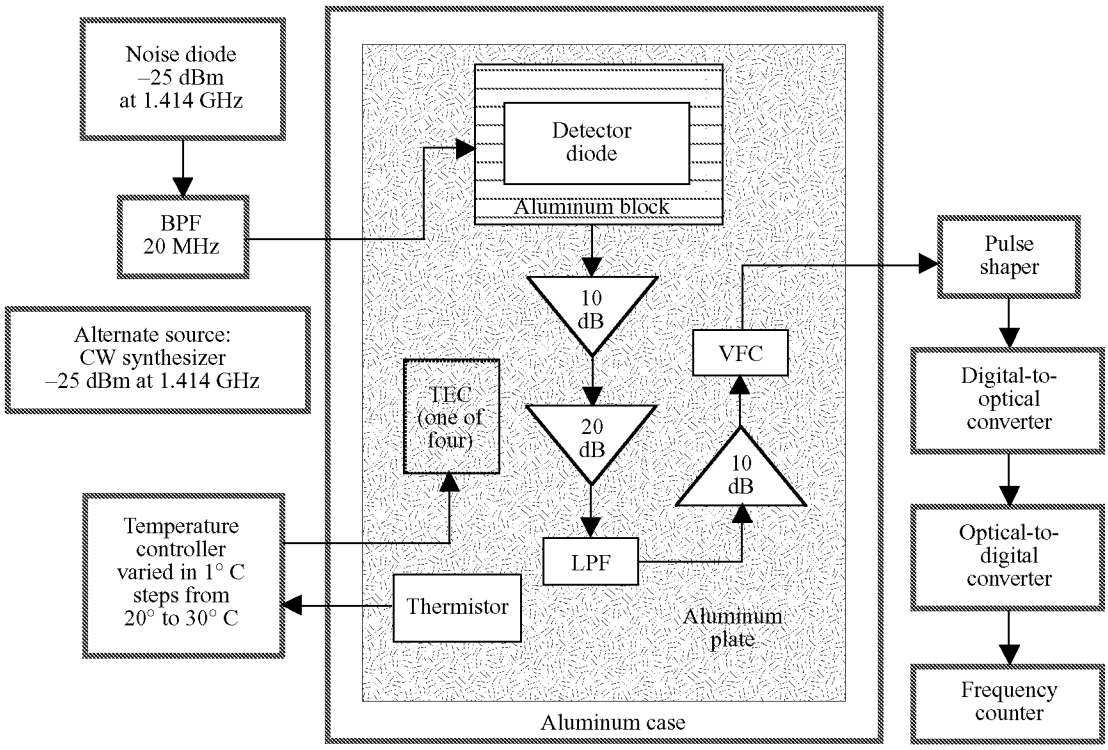

Figure 2. Experimental setup for measuring the thermal coefficient of the diode/VFC. The coefficient was calculated from the change in output frequency versus change in physical temperature of the detector, for a constant input power.

temperature, the same input power of –25 dBm was applied and the output was recorded in kilohertz. Frequency and physical temperature data were recorded by hand.

The test was performed with a 1.414-GHz noise diode and repeated using a 1.414-GHz sine wave synthesizer as the source. The noise diode produced noise uniformly distributed across a 20-MHz bandwidth and Gaussian-distributed in amplitude. Thus the rms noise voltage was one-third of its peak voltage. In contrast, the sine wave rms voltage was 0.707 times its peak voltage. A gain curve was obtained at the beginning of each test by inputting a series of power levels from 2.0 to 4.5 μW, as indicated by a power meter, and recording the detector output in kilohertz. Information for the gain curves was collected with the diode/VFC detector at 25°C, the midpoint of the temperature range of interest. This temperature was chosen because it was a likely candidate for operation in a radiometer. Gain was then calculated in MHz/mW; the gain figure was later used to calculate the thermal coefficient in terms of W/°C.

Setup and Measurement Procedure for the Flash ADC Detector Test

The experimental setup for the flash ADC thermal test is shown in a block diagram in figure 3. Appendix B lists more detailed part and instrument names.

The 8-bit flash ADC evaluation kit contained two test points with current-to-ground ratios proportional to the die physical temperature. These currents, named I_{PTAT} and I_{CONST}, were monitored with an ammeter as the ADC temperature was allowed to rise slowly. With the ambient room temperature at

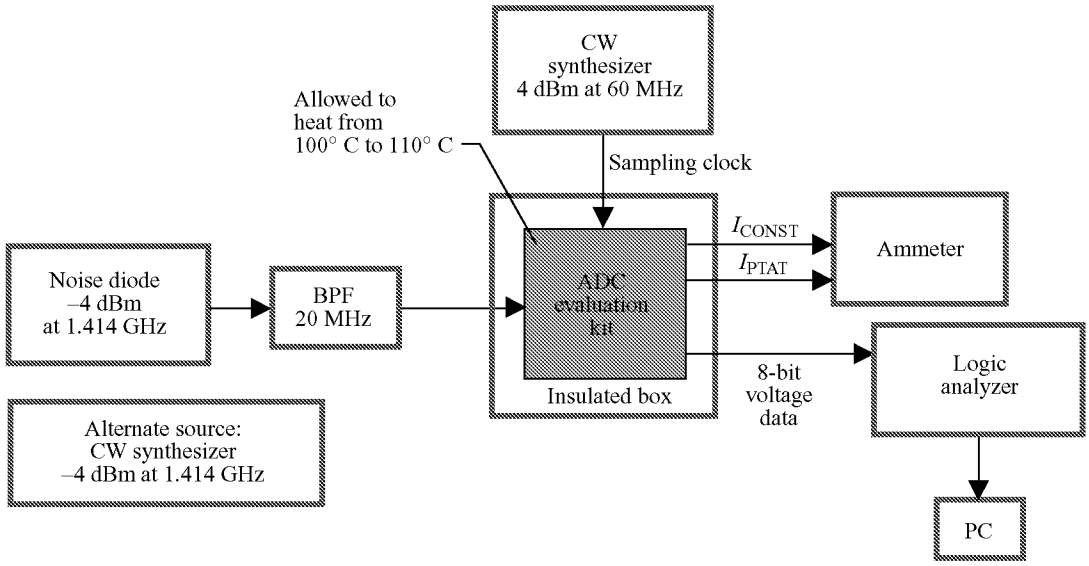

Figure 3. Experimental setup for measuring the thermal coefficient of the flash ADC detector. I_{CONST} and I_{PTAT} were currents built into the ADC chip to allow calculation of the die physical temperature. These currents, together with the digital voltage data, were recorded as the insulated box slowly heated the ADC die from 100° to 110°C. The coefficient was calculated from the change in output counts^2 versus change in physical temperature of the detector, for a constant input power.

25°C, the initial die temperature was 100°C. An insulated box was placed over the ADC, and the ADC was allowed to warm itself gradually until its die temperature had reached 110°C.

A CW synthesizer provided the ADC sampling clock signal, which was a 60-MHz sine wave. For bandpass sampling of noise with 20 MHz of bandwidth, a sampling frequency of at least 2.5 times the bandwidth, or 50 MHz, was required. At the chosen sampling frequency of 60 MHz, noise at 1.414 GHz ± 10 MHz was downconverted to an intermediate frequency band from 16 to 30 MHz.

The ADC was configured to operate in DIV2 mode, in which the output data rate equaled half the sampling clock rate. The 16 data output lines of the ADC were connected to a logic analyzer, and pairs of 8-bit bytes of 60-MHz data were output at 30 MHz. At approximately 0.5° intervals, voltage data collected by the logic analyzer were dumped to a PC through a GPIB until 10 sets of 992 samples had been collected at each temperature. These groups of 9920 samples represented sampling periods of about 2.5 min. At each temperature, the same input power of –4 dBm was applied and the detector output was calculated in rms counts^2. Temperature and counts^2 data were recorded by hand.

The test was performed using a 1.414-GHz noise diode and repeated using a 1.414-GHz sine wave synthesizer as the source. A gain curve was obtained at the beginning of each test by inputting a series of power levels from 0 W to 0.5 mW and calculating the detector output in counts^2. Information for the gain curves was collected with the ADC detector at 100°C, the lower end of the temperature range of interest. Like the diode/VFC tests, this temperature range was chosen because it was a likely candidate for operation in a radiometer. Gain was then calculated in counts^2/mW; the gain figure was later used to calculate the thermal coefficient in terms of W/°C.

Calculations for the Diode/VFC Detector Test

The next three sections explain the calculations performed for the diode/VFC detector thermal test.

Root Mean Square Power

The detector VFC output a series of digital pulses, which were counted over intervals of 100 sec by a frequency counter. From the slope of the gain curve, a linear correspondence was obtained between hertz and watts. The average frequency obtained by the counter could then be translated into the rms power measured by the detector.

Thermal Coefficient of the Detector

The thermal response curve of the detector (as seen in figs. 8–11) provided a slope in Hz/°C. Taking into account the slope and the offset of the gain curve, the thermal coefficient was calculated in ppt/°C as follows:

$$(\mathrm{TC})_{\mathrm{ppt/^\circ C}} = \frac{(\mathrm{TC})_{\mathrm{Hz/^\circ C}}}{(\mathrm{Output\ at\ 25^\circ C})_{\mathrm{Hz}} - (\mathrm{Offset\ at\ 25^\circ C})_{\mathrm{Hz}}} \tag{1}$$

The thermal coefficient of the detector in W/°C was calculated from the thermal coefficient in Hz/°C and the detector gain in Hz/W:

$$(\mathrm{TC})_{\mathrm{W/^\circ C}} = \frac{(\mathrm{TC})_{\mathrm{Hz/^\circ C}}}{G_{\mathrm{Hz/W}}} \tag{2}$$

Thermal Coefficient for an Example Radiometer

To predict the effect of the diode/VFC detector thermal sensitivity on a radiometer measurement of brightness temperature, an example application was formulated for sea surface salinity. The brightness temperature of the sea surface is approximately 100 K. Allowing 300 K for the radiometer system temperature and 20 MHz of bandwidth, the power into the radiometer would be $k_{\mathrm{Boltzmann}}\,\mathrm{TB}$ or

$$P_{\mathrm{in}} = (1.381 \times 10^{-23}\ \mathrm{J/K})(400\ \mathrm{K})(20\ \mathrm{MHz}) = -99.57\ \mathrm{dBm} \tag{3}$$

To amplify the input power sufficiently to be detected by the diode, the required front-end gain would be

$$G_{\mathrm{front\text{-}end}} = -25\ \mathrm{dBm} - (-99.57\ \mathrm{dBm}) = 74.57\ \mathrm{dB} \tag{4}$$

The change in the radiometer output per degree change of the detector would be calculated as

$$(\mathrm{TC})_{\mathrm{K/^\circ C}} = (\mathrm{TC})_{\mathrm{W/^\circ C}}\left(\frac{1}{k_{\mathrm{Boltzmann}}\mathrm{B}}\right)\left(\frac{1}{G_{\mathrm{front\text{-}end}}}\right) = (\mathrm{TC})_{\mathrm{W/^\circ C}}(1.264 \times 10^{8})\mathrm{K/W} \tag{5}$$

Calculations for the ADC Detector Test

The next three sections explain the calculations performed for the ADC detector thermal test.

Root Mean Square Power

The ADC detected voltage between 0 and 256 counts. Each time 9920 voltage samples were collected, their mean was computed and subtracted from each value to obtain a series of dc voltage values in counts. These values were squared and averaged to obtain an rms value for power in $counts^2$. After 10 of these series had been collected, the average rms power was calculated for the whole 2.5 min of data.

Thermal Coefficient of the Detector

The temperature response curve of the detector provided a slope in $counts^2/°C$. Taking into account the slope and the gain curve offset, the thermal coefficient was calculated in ppt/°C as follows:

$$(TC)_{ppt/°C} = \frac{(TC)_{counts^2/°C}}{(\text{Output at } 105°C)_{counts^2} - (\text{Offset at } 100°C)_{counts^2}} \tag{6}$$

The thermal coefficient of the detector in W/°C was calculated from the thermal coefficient in $counts^2/°C$ and the detector gain in $counts^2/W$:

$$(TC)_{W/°C} = \frac{(TC)_{counts^2/°C}}{G_{counts^2/W}} \tag{7}$$

Thermal Coefficient for an Example Radiometer

To determine the effect of the ADC detector thermal temperature sensitivity on a radiometer measurement of brightness temperature, the same example was used as for the diode/VFC detector. As explained in the section "Calculations for the Diode/VFC Detector Test," the input power for the radiometer was –99.57 dBm. To amplify the input power sufficiently to be detected by the ADC, the required front-end gain would be

$$G_{\text{front-end}} = -4.0 \text{ dBm} - (-99.57 \text{ dBm}) = 95.57 \text{ dB} \tag{8}$$

The change in the radiometer output per degree change of the detector would be calculated as

$$(TC)_{K/°C} = (TC)_{W/°C}\left(\frac{1}{k_{Boltzmann}B}\right)\left(\frac{1}{G_{\text{front-end}}}\right) = (TC)_{W/°C}(1.004 \times 10^6)_{K/W} \tag{9}$$

Results and Observations

Gain Curves

Table 1 shows the average gains calculated from all tests on each detector, with L-band noise as input and with an L-band sine wave as input. For the diode/VFC detector, the sine wave input produced a smaller gain than the noise input (443 MHz/mW versus 493 MHz/mW). For the flash ADC detector, the sine wave input produced a larger gain than the noise input (9516 $counts^2$/mW versus 8971 $counts^2$/mW). These differences appear significant, and it may be that the detectors under test saw the input powers differently from the power meter, which read the two sources as having the same rms

power. However, as the tests were performed on different days and the cabling had been completely disassembled and reassembled between noise and sine wave input tests for the same detector, no firm conclusions may be drawn from the gain differences alone.

Table 1. Measured Detector Gains

Source	Diode/VFC gain, MHz/mW	Flash ADC gain, counts^2/mW
Noise diode	493.49 ± 3.34	8971 ±± 72
Sine wave synthesizer	443.02 ± 0.37	9516 ± 38

Figures 4 and 5 show representative gain curves for the diode/VFC and ADC detectors, respectively, with an L-band noise input. The diode/VFC curve was quite linear and had a frequency axis intercept near –500 kHz. This offset frequency was due to a small amplifier voltage present at the op amp input regardless of inputs from the detector diode. The ADC detector gain curve was somewhat less linear than the diode/VFC detector curve. It crossed the counts^2 axis close to zero; the small offset was probably due to noise caused by timing errors in the logic analyzer sampling. Figures 6 and 7 show

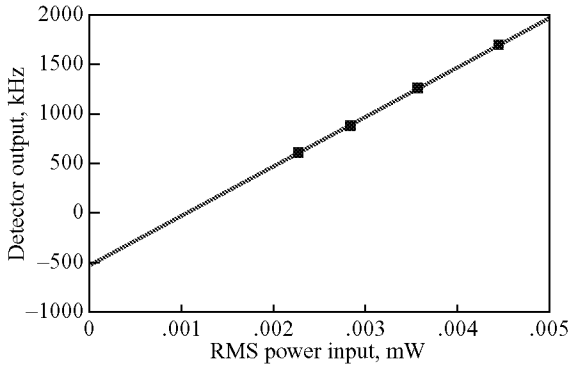

Figure 4. Representative gain curve for the diode/VFC detector with noise input. Thermal tests performed at 0.0031 mW (–25 dBm); G = 496.75 MHz/mW; 08/22/00b.

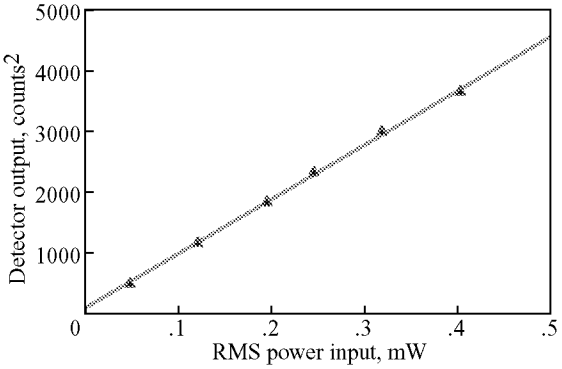

Figure 5. Representative gain curve for the ADC detector with a noise input. Thermal tests performed at 0.398 mW (–4 dBm); G = 8872.2 counts^2/mW; 9/08/00b.

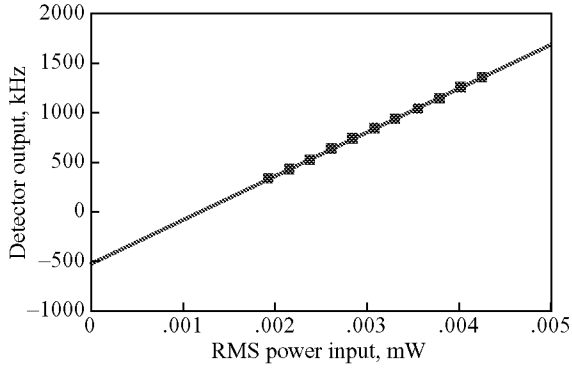

Figure 6. Representative gain curve for diode/VFC detector with a sine wave input; G = 442.9 MHz/mW; 08/18/00.

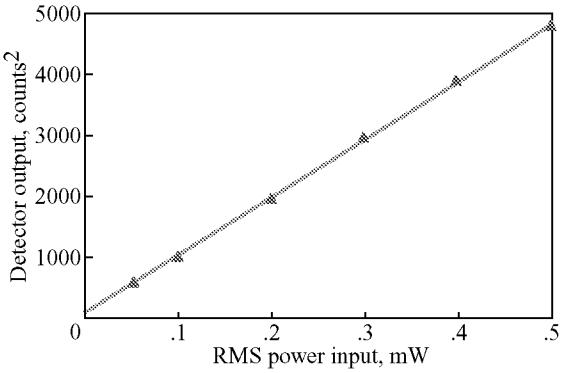

Figure 7. Representative gain curve for the ADC detector with a sine wave input; G = 9476.3 counts^2/mW; 10/02/00.

representative gain curves for the diode/VFC and ADC detectors, respectively, with an L-band sine wave input. Again, both responses were linear. However, as mentioned above, the gains were somewhat different from those obtained with noise inputs.

Thermal Coefficients of the Detectors

Table 2 gives the average of the thermal coefficient test results for the two detectors; each average represents at least three tests. The thermal coefficients have been calculated by the methods described earlier in the sections "Calculations for the Diode/VFC Detector Test" and "Calculations for the ADC Detector Test." A gain was computed immediately prior to each thermal test. Taking into account the (chronologically) closest gain to compute the change in detected power per change in °C, we see that the thermal coefficient for the diode/VFC detector was not significantly different with a sine wave input than with a noise input (3.37 nW/°C versus 3.52 nW/°C). For the ADC detector, however, the absolute thermal coefficient was much less with a sine wave input than with a noise input (−0.814 μW/°C versus −1.13 μW/°C). The only difference that could explain this behavior is the higher maximum voltage of the noise input, compared with a sine wave input with the same rms value. For either input, we see that the absolute thermal coefficient in ppt/°C is about twice as high for the flash ADC as for the diode/VFC detector (−2.93 ppt/°C versus 1.24 ppt/°C or −2.03 ppt/°C versus 1.12 ppt/°C).

Table 2. Measured Thermal Coefficients

Source	Diode/VFC thermal coefficient	Flash ADC thermal coefficient
Noise diode	1.74 ± 0.15 kHz/°C	−10.19 ± 1.44 counts^2/°C
	3.52 ± 0.28 nW/°C	−1.13 ± 0.16 μW/°C
	1.24 ± 0.10 ppt/°C at 25°C	−2.93 ± 0.29 ppt/°C at 105°C
Sine wave synthesizer	1.49 ± 0.17 kHz/°C	−7.75 ± 1.42 counts^2/°C
	3.37 ± 0.39 nW/°C	−0.814 ± 0.148 μW/°C
	1.12 ± 0.13 ppt/°C at 25°C	−2.03 ± 0.39 ppt/°C at 105 °C

The data sheet for the MICA diode detector under test did not give thermal sensitivity values, but data sheets for similar planar-doped detector diodes manufactured by Agilent Technologies and Metelics Corporation showed their sensitivity as 3 ppt/°C and 3.23 ppt/°C, respectively. From Burr-Brown Corporation data sheets, the amplifiers in the diode/VFC detector (as shown by fig. 2 and appendix A) were estimated to contribute 0.001 ppt/°C, 0.071 ppt/°C, 0.001 ppt/°C, and 0.026 ppt/°C. The VFC gain drift was estimated at 0.050 ppt/°C. From the root-sum-square of all these, the resulting typical thermal sensitivity of the detector was expected to be 3.116 ppt/°C. The test device therefore performed better than expected. Maxim Integrated Products described the ADC as having a 0.150 ppt/°C input resistance temperature coefficient and an on-chip voltage reference temperature coefficient of 0.024 ppt/°C. From the root-sum-square of these two values, the MAX106 ADC evaluation kit was expected to have a thermal sensitivity of at least 0.152 ppt/°C. The measured thermal coefficient was 2 to 3 ppt/°C, depending on the input type.

Shown in figures 8 through 11 are representative thermal coefficient test results for the two detectors. Figures 8 and 9 show the output change per degree Celsius for the diode/VFC and ADC detectors, respectively, when the source was a noise diode. Figures 10 and 11 show the output change per degree Celsius for the same detectors when the source was a sine wave synthesizer. The results in all cases showed a linear change with temperature, the coefficient being positive for the diode/VFC detector and negative for the ADC detector. For the diode/VFC detector, a similar result was obtained with either source. For the ADC detector, the thermal coefficient was significantly larger with the noise source.

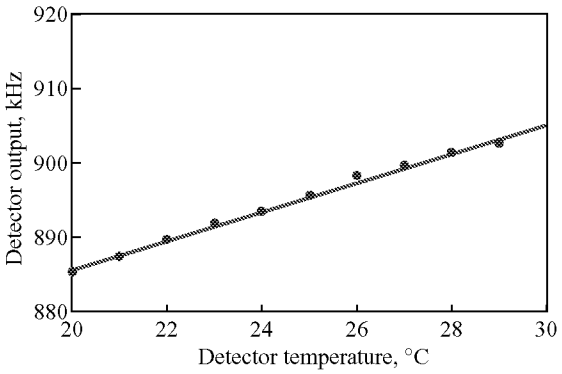

Figure 8. Representative thermal coefficient curve for the diode/VFC detector with a –25 dBm noise input; TC = 1.9390 kHz/°C; 08/22/00b.

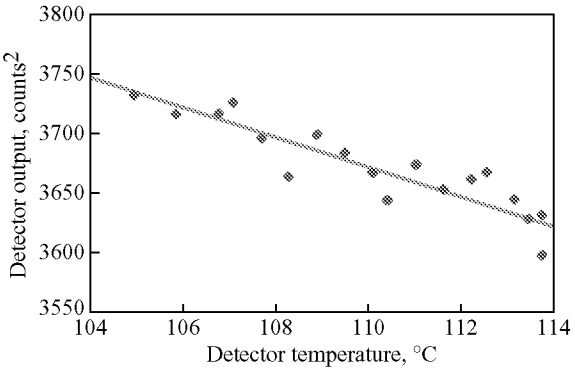

Figure 9. Representative thermal coefficient curve for the ADC detector with a –4 dBm noise input; TC = –12.561 counts^2/°C; 09/08/00b.

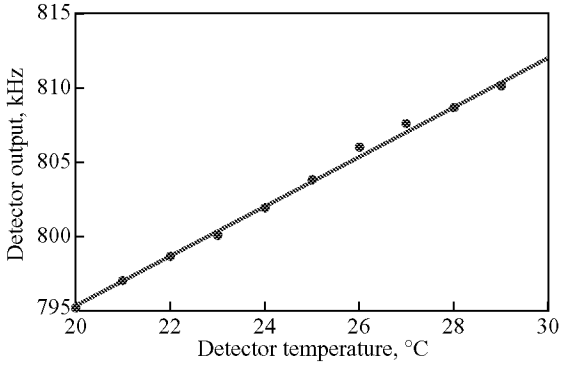

Figure 10. Representative thermal coefficient curve for the diode/VFC detector with a –25 dBm sine wave input; TC = 1.6636 kHz/°C; 08/18/00.

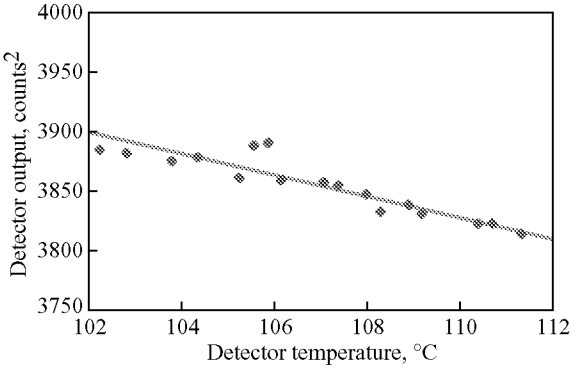

Figure 11. Representative thermal coefficient curve for the ADC detector with a –4 dBm sine wave input; TC = –8.9333 counts^2/°C; 10/02/00.

The scatter in test results was much higher for the flash ADC than for the diode/VFC. This difference was due to the test setup. The diode/VFC detector was borrowed from a radiometer under construction and was mounted in a temperature-controlled case. Because no special temperature-controlled chamber had been constructed for the ADC, its temperature varied more than that of the diode/VFC detector during the time periods when output data were being collected. Also, the ADC was not well shielded and had many long test leads that could pick up noise.

The ADC tests were repeated over a variety of clock frequencies (60 MHz ± 2 MHz) to determine if the thermal response was clock frequency dependent. No significant change in thermal coefficient was noted with change in the clock frequency. However, a very significant change did result from using different input power levels. For example, the thermal coefficient increased from –7.75 counts^2/°C at –4 dBm to –24.40 counts^2/°C at –1 dBm. For the purposes of this study, it was (somewhat arbitrarily) decided to conduct the thermal tests at –4 dBm so that the available ADC range would be approximately 70 percent occupied by the peak-to-peak input. In fairness to the ADC, it should be restated that the ADC performance was related to the input frequency. Given that the gain of the ADC was 3 dB more at 0 Hz than at 1.414 GHz, presumably the thermal coefficient would also be less for dc inputs than for L-band inputs.

Contribution to the Measurement Error of a Radiometer

Because different thermal coefficients were found for the flash ADC detector depending on input type, and because a radiometer is a noise detector, the estimated radiometer measurement error was computed using the noise input thermal coefficient only. From the results of the thermal tests on each detector using a 1.414-GHz noise diode as input, the error was computed as shown in table 3. For a −25 dBm input to the diode/VFC detector at 25°C and a −4 dBm input to the ADC detector at 105°C, these results show how the brightness temperature measurement would change with each degree Celsius change in the detector. The ADC contribution to brightness temperature error would be about 2.8 times more than the diode/VFC contribution.

Table 3. Thermal Coefficient Contribution to Error in a Sea Surface Radiometer

Source	Diode/VFC thermal coefficient at 25°C, K/°C	Flash ADC thermal coefficient at 105°C, K/°C
Noise	0.40 ± 0.03	-1.12 ± 0.16

Concluding Remarks

This study was conducted with physical temperatures and input powers reasonable for a radiometer. The chief findings of this study were:

1. At the physical temperature ranges and input power levels tested, the diode/VFC (voltage-to-frequency converter) detector was less sensitive to thermal change than the flash ADC (analog-to-digital converter) detector by a factor of 2.8. Therefore, based on considerations of thermal stability alone, the ADC did not offer an advantage when incorporated into an L-band radiometer.

2. The diode/VFC detector exhibited a positive thermal coefficient, while the flash ADC detector exhibited a negative thermal coefficient.

3. For the diode/VFC detector, the thermal coefficient test gave the same results with a noise input or a sine wave input.

4. For the flash ADC detector, the thermal coefficient test gave different results depending on the input type. Therefore, tests on a flash ADC should be performed with the same input type as will be used in the application.

A limitation of the study was that the ADC was tested while mounted on an evaluation kit circuit board provided by the manufacturer. It is possible that different results could be obtained by building a more permanent assembly to contain the ADC.

References

1. Blume, Hans-Juergen C.; Kendall, Bruce M.; and Fedors, John C.: Measurement of Ocean Temperature and Salinity Via Microwave Radiometry. *Boundary-Layer Meteorology*, Vol. 13, D. Reidel Publ. Co., 1978, pp. 295–308.

2. Scherner, M. J.; and Lawrence, R. W.: *Noise Diode Stability Measurements Using a 4.3 GHz Laboratory Radiometer*. NASA TM-112865, 1997.

3. Mackenzie, Anne I.; and Lawrence, Roland W.: *Three Averaging Techniques for Reduction of Antenna Temperature Variance Measured by a Dicke Mode, C-Band Radiometer*. NASA/TM-2000-210283, 2000.

4. Lawrence, R. W.; and Campbell, T. G.: Radiometric Characterization of Mesh Reflector Material for Deployable Real Aperture Remote Sensing Applications. *IEEE 2000 International Geoscience and Remote Sensing Symposium*, July 2000, pp. 2724–2726.

5. Tanner, Allen B.: Development of a High-Stability Water Vapor Radiometer. *Radio Sci.*, vol. 33, no. 2, Mar.–Apr. 1998, pp. 449–462.

6. Tempel, R.; Lütke, W.; Herrmann, J.; and Wolff, I.: MMICs for Sensor Applications. *IEEE 1996 Microwave and Millimeter-Wave Monolithic Circuits Symposium*, 1996, pp. 209–212.

7. Shoucri, Merit; Dow, G. Samuel; Fornaca, Steven; Hauss, Bruce; and Yujiri, Larry: Passive Millimeter Wave Camera for Enhanced Vision Systems. *SPIE Proc.*, Vol. 2, 1996, pp. 2–8.

8. Fischman, Mark A.; and England, Anthony W.: Sensitivity of a 1.4 GHz Direct-Sampling Digital Radiometer. *IEEE Trans. Geosci. & Remote Sensing*, vol. 17, no. 5, Sept. 1999, pp. 2172–2180.

9. Akos, Dennis M.; and Tsui, James B. Y.: Design and Implementation of a Direct Digitization GPS Receiver Front End. *IEEE Trans. Microwave Theory & Tech.*, vol. 44, no. 12, pt. 2, Dec. 1996, pp. 2334–2339.

Appendix A

Parts and Instrument List for Diode/VFC Test

The following is a list of parts and instruments used for the diode/VFC test:

Noise Source: Microwave Semiconductor Solid State Noise Source MC65189

Sine Wave Source: Hewlett-Packard 83712B Synthesized CW Generator

Detector Diode: MICA Microwave DTN 4080 M1

1st 10 dB Op Amp: Burr-Brown PGA 207P

20 dB Op Amp: Burr-Brown OPA 2132

Lowpass Filter Op Amp: Burr-Brown OPA 2132

2nd 10 dB Op Amp: Burr-Brown INA 111

Voltage-to-Frequency Converter: Burr-Brown VFC 110

Pulse Shaper/Buffer: National Semiconductor DS75451

Digital-to-Optical Converter: Hewlett-Packard HFBR-1412

Optical-to-Digital Converter: Hewlett-Packard HFBR-2412

Hewlett-Packard 5345 Frequency Counter

Temperature Controller: ILX Lightwave LDT-5910B

Thermoelectric Cooler: Melcor Polar TEC PT4-7-30

Power Meter: Boonton 4200 RF Microwattmeter

Appendix B

Parts and Instrument List for Flash ADC Test

The following is a list of parts and instruments used for the flash ADC test:

Noise Source: Microwave Semiconductor Solid State Noise Source MC65189

Sine Wave Source: Hewlett-Packard 83712B Synthesized CW Generator

Clock Signal Source: Hewlett-Packard 8656B Signal Generator

ADC Detector: MAXIM MAX106 Analog-to-Digital Evaluation Kit

Logic Analyzer: Gould Biomation K100-D

Ammeter: Agilent 34401A

Power Meter: Boonton 4200 RF Microwattmeter

PC with LabVIEW Software

REPORT DOCUMENTATION PAGE

Form Approved
OMB No. 0704-0188

1. AGENCY USE ONLY *(Leave blank)*	2. REPORT DATE	3. REPORT TYPE AND DATES COVERED
	December 2001	Technical Memorandum

4. TITLE AND SUBTITLE
Comparison of Thermal Coefficients for Two Microwave Detectors
Diode/Voltage-to-Frequency Converter and Flash Analog-to-Digital Converter

5. FUNDING NUMBERS
WU 258-80-00-32

6. AUTHOR(S)
Anne I. Mackenzie

7. PERFORMING ORGANIZATION NAME(S) AND ADDRESS(ES)
NASA Langley Research Center
Hampton, VA 23681-2199

8. PERFORMING ORGANIZATION REPORT NUMBER
L-18091

9. SPONSORING/MONITORING AGENCY NAME(S) AND ADDRESS(ES)
National Aeronautics and Space Administration
Washington, DC 20546-0001

10. SPONSORING/MONITORING AGENCY REPORT NUMBER
NASA/TM-2001-211258

11. SUPPLEMENTARY NOTES

12a. DISTRIBUTION/AVAILABILITY STATEMENT
Unclassified–Unlimited
Subject Category 35 Distribution: Standard
Availability: NASA CASI (301) 621-0390

12b. DISTRIBUTION CODE

13. ABSTRACT ***(Maximum 200 words)***

Laboratory measurements were performed to compare the thermal coefficients of two microwave detectors that might be used for direct detection in L-band radiometers. In particular it was desired to compare the performance of a new-technology flash ADC (analog-to-digital converter) against that of an older-technology diode detector in series with a VFC (voltage-to-frequency converter). The outputs of two state-of-the-art detectors were recorded as a constant 1.414-GHz signal was input and the physical temperatures of the detectors were varied over a range of 10°C. As a further experiment, each detector was tested with a noise diode source and with a sine wave synthesizer source. Thermal coefficients were computed in terms of W/°C and in terms of ppt/°C at nominal operating temperatures reasonable for the individual devices. Finally, thermal coefficients were calculated in K/°C to indicate the change in brightness temperature seen by a theoretical sea surface salinity radiometer employing each detector. The K/°C for the flash ADC was determined to be about 2.8 times that of the diode/VFC. Different reactions of the ADC to a noise input and a sine wave input indicated that ADC tests for radiometric purposes, such as this one, should be performed using a noise input.

14. SUBJECT TERMS	15. NUMBER OF PAGES
Radio frequency; Radiometer; Microwave; Millimeter wave; Direct detection; Analog-to-digital converter; Detector diode; Thermal coefficient; Stability	22
	16. PRICE CODE

17. SECURITY CLASSIFICATION OF REPORT	18. SECURITY CLASSIFICATION OF THIS PAGE	19. SECURITY CLASSIFICATION OF ABSTRACT	20. LIMITATION OF ABSTRACT
Unclassified	Unclassified	Unclassified	UL